

Neural Architecture Search Using Stable Rank of Convolutional Layers

Kengo Machida¹, Kuniaki Uto¹, Koichi Shinoda¹, Taiji Suzuki^{2,3}

¹Tokyo Institute of Technology, Japan

²Graduate School of Information Science and Technology, The University of Tokyo, Japan

³Center for Advanced Intelligence Project, RIKEN, Japan

machida@ks.c.titech.ac.jp, uto@ks.c.titech.ac.jp, shinoda@c.titech.ac.jp, taiji@mist.i.u-tokyo.ac.jp

Abstract

In Neural Architecture Search (NAS), Differentiable ARchiTecture Search (DARTS) has recently attracted much attention due to its high efficiency. It defines an over-parameterized network with mixed edges each of which represents all operator candidates, and jointly optimizes the weights of the network and its architecture in an alternating way. However, this process prefers a model whose weights converge faster than the others, and such a model with fastest convergence often leads to overfitting. Accordingly the resulting model cannot always be well-generalized. To overcome this problem, we propose Minimum Stable Rank DARTS (MSR-DARTS), which aims to find a model with the *best generalization error* by replacing the architecture optimization with the selection process using the minimum stable rank criterion. Specifically, a convolution operator is represented by a matrix and our method chooses the one whose stable rank is the smallest. We evaluate MSR-DARTS on CIFAR-10 and ImageNet dataset. It achieves an error rate of 2.92% with only 1.7M parameters within 0.5 GPU-days on CIFAR-10, and a top-1 error rate of 24.0% on ImageNet. Our MSR-DARTS directly optimizes an ImageNet model with only 2.6 GPU days while it is often impractical for existing NAS methods to directly optimize a large model such as ImageNet models and hence a proxy dataset such as CIFAR-10 is often utilized.

1 Introduction

Neural Architecture Search (NAS) seeks to design neural network structure automatically, and has already been successful on many tasks (Ahn, Kang, and Sohn 2018; Liu et al. 2019; Pham et al. 2018). In NAS, all possible architectures are defined by a *search space*, which consists of network topologies and operator sets, and a *search strategy* is used to obtain a better architecture efficiently on the defined search space. As a recent trend in the search space, a small component in a network called *cell* are defined as an optimization target to reduce search cost. For search strategy, Reinforcement Learning (RL) (Zoph and Le 2017; Zoph et al. 2018; Pham et al. 2018) and Evolutionary Algorithms (EA) (Liu et al. 2018b; Tang, Golbabaei, and Davies 2017; Real et al. 2019) are widely used.

Recently, DARTS (Liu, Simonyan, and Yang 2019) and its derivations (Xie et al. 2019; Chen et al. 2019; Xu et al. 2019; Liang et al. 2019) proposed differentiable approaches which relax the search spaces to be continuous and thus enable direct application of gradient based optimization. These methods are effective in the search cost since they skip the evaluation of each sampled architecture, which is required in RL and EA. The cell defined in these works is Direct Acyclic Graph (DAG) with multiple nodes, each of which is a latent representation (*e.g.*, a feature map in convolutional networks) and each directed edge is associated with an operator. While these works explicitly introduce *architecture parameters* as learnable parameters in addition to the weight parameters of over-parameterized networks in the architecture search, each edge in DAG is a *mixed edge* which includes all candidate operators in the operator set and each operator is weighted by an architecture parameter. An architecture parameter indicates how suitable its operator in a mixed edge is. The architecture parameters are jointly trained with the weight parameters in an alternating way. However, it is reported that this optimization process tends to produce a fast converge architecture, which is not always the optimal solution in terms of accuracy (Shu, Wang, and Cai 2020).

We propose a new pipeline named Minimum Stable Rank Differentiable ARchiTecture Search (MSR-DARTS) to solve this problem. In this method, the optimization of the learnable architecture parameters is replaced with the selection process using stable rank criterion and thus only weight parameters of neural networks are trained during the architecture search. The discrete architecture is derived by assuming that only limited convolutional operators (*e.g.*, separable convolution and dilated convolution with different kernel size) are included in our operator set, in which each convolutional operator is regarded as a matrix. Then we utilize the stable rank (numerical rank) of each convolution to derive a discrete architecture. Specifically, in each mixed edge, the operator which has the lowest stable rank is selected. The architecture search based on the stable rank is appropriate considering that the low rankness of matrix is related to the generalization ability of neural networks. Several studies (Arora et al. 2018; Suzuki, Abe, and Nishimura 2020) reported that a neural network with lower stable rank operators gets a higher generalization ability, where a stable rank is often used instead of a rank because the former properly captures

the statistical degrees of freedom by ignoring negligibly tiny singular values. More precisely, when an input is noisy, a low stable rank convolution conveys the input information only and attenuates noise. Thus, a network with low stable rank has better generalization ability and is robust against noisy input. In summary, we train an over-parameterized network with fixed architecture parameters and thus only the weights of the network are optimized. Then, the discrete architecture is derived by using stable rank of each operator by treating a convolution as a matrix in MSR-DARTS to yield a well generalized architecture.

We conducted experiments with CIFAR-10 and ImageNet dataset. Our proposed approach achieves an error rate of 2.92% with only 1.7 M parameters on CIFAR-10 and a top-1 error rate of 24.0% on ImageNet. Results on CIFAR-10 is competitive with the 1st order DARTS while the number of parameters in the MSR-DARTS is reduced to 50% of those in the DARTS. It is often impractical for NAS to directly optimize a large model such as ImageNet models, and hence, a proxy dataset such as CIFAR-10 is often utilized. Our MSR-DARTS directly optimizes an ImageNet model and achieves slightly better than recently proposed PC-DARTS with only 2.6 GPU days, with 24% search cost reduction.

2 Related Work

2.1 Neural Architecture Search

There has been growing interest in NAS since (Zoph and Le 2017) proposed its algorithm. In early years, EA and RL are used to optimize network architectures. The algorithm using RL trains a recurrent neural network meta-controller to guide the search process, and it gradually samples a better architecture. (Zoph et al. 2018; Pham et al. 2018) first optimize the structure of a small component in an entire network, namely a cell, instead of the entire network structure, and then the entire network is constructed by stacking the optimized cells. This two step process reduces the search cost. (Liu et al. 2018b; Tang, Golbabaei, and Davies 2017; Real et al. 2019) utilized EAs, which mutate the architecture topologies and evolve towards better performances. DARTS introduced a differentiable NAS pipeline, which relaxes the search space to be continuous and directly uses gradient based optimization. Many works (Xie et al. 2019; Chen et al. 2019; Xu et al. 2019; Liang et al. 2019) follow this approach and achieve remarkable performance with improved efficiency.

2.2 Generalization Error Analysis

A deep network generalizes well even when it has a larger amount of parameters than the sample size. Generalization bounds represent the upper bound of the generalization error. We can guarantee that a model with small training error can have a high generalization performance if the generalization error (difference between training error and expected error) can be evaluated properly and has a small upper bound. There are several metrics to represent generalization error bounds such as VC-dimension (Vapnik 1998; Harvey, Liaw, and Mehrabian 2017), PAC-Bayes theory (Neyshabur, Bhojanapalli, and Srebro 2017; Dziugaite and Roy 2017), norm

based analysis (Bartlett and Mendelson 2002; Neyshabur, Salakhutdinov, and Srebro 2015; Golowich, Raklin, and Shamir 2018), and compression based approach (Arora et al. 2018; Baykal et al. 2019; Suzuki, Abe, and Nishimura 2020). Among them, the compression based approach has recently attracted much attention because it gives tighter generalization error bounds for deep neural networks. For example, (Arora et al. 2018) uses the low rank property of weight matrices to compress neural networks based on the fact that a matrix with a lower stable rank is more robust to noise thus generalizes well. (Suzuki, Abe, and Nishimura 2020) experimentally confirmed that most networks have near low rank weight matrices after training, where a near low rank matrix is defined as a matrix in which a small number of singular values are significantly large while the other singular values are close to zero. This near low rank property is used to derive generalization bounds.

2.3 DARTS

In this study, similar to (Xie et al. 2019; Chen et al. 2019; Xu et al. 2019), we use DARTS as a baseline framework. DARTS stacks L cells, each of which is represented as a DAG of an ordered sequence of N nodes, $\{x_0, x_1, \dots, x_{N-1}\}$, where each node x_i is a feature map and each edge (i, j) ($i < j$) denotes an information flow from node i to node j . A set of K candidate operators is denoted by $\mathcal{O} = \{o_0, o_1, \dots, o_{K-1}\}$, in which an element o_v which includes a learnable parameter $w_v^{(i,j)}$ is the v -th candidate operator defined in advance (e.g., separable convolution and dilated convolution). Figure 1 left illustrates an example of a DAG with 4 nodes. An information flow between nodes is a mixed edge which includes all of candidate operators. An architecture parameter $\alpha_v^{(i,j)}$, which indicates how suitable the v -th candidate operator is for mixed edge (i, j) , is introduced as a weight for o_v . The goal is to optimize $\alpha_v^{(i,j)}$ ($v = 0, \dots, K-1$). For each $i < j$, the information flow from node i to node j , illustrated in the middle top of Figure 1, is computed as:

$$f_{i,j}(x_i) = \sum_{v=0}^{K-1} \frac{\exp(\alpha_v^{(i,j)})}{\sum_{v'=0}^{K-1} \exp(\alpha_{v'}^{(i,j)})} \cdot o_v(x_i). \quad (1)$$

An output of node j is a sum over all information flows from its predecessors

$$x_j = \sum_{i < j} f_{i,j}(x_i). \quad (2)$$

The first two nodes, x_0 and x_1 , are input nodes to a cell. The output of all the cells equals to the output of the final node x_{N-1} , which is defined as the concatenation of all the intermediate cells, i.e., $\text{concat}(x_2, x_3, \dots, x_{N-2})$.

There are two types of cells introduced in DARTS. One is normal cell which keeps the spatial resolution, and the other is reduction cell which reduces the spatial resolution of feature maps. Note that while DARTS shares the architecture topology among all normal cells, the same is true for reduction cells, because it optimizes architecture parameters ($\alpha_{\text{normal}}, \alpha_{\text{reduce}}$), where α_{normal} is shared by all the normal cells and α_{reduce} is shared by all the reduce cells.

DARTS has two stages. The first stage is a search stage, which trains the over-parameterized network which consists of mixed edges in each of which all possible operators are included, and derives a promising discrete architecture according to the architecture parameter $\alpha_v^{(i,j)}$ (See Subsec. 3.4 for more details). The second stage is an evaluation stage which trains the derived architecture from full-scratch.

3 Method

3.1 MSR-DARTS

While DARTS and many related works (Xie et al. 2019; Chen et al. 2019; Xu et al. 2019) search architectures by jointly training architecture parameters α and weights of neural networks w (e.g., the parameters of convolutional operator) in an alternating way ($\alpha_v^{(i,j)}$ is denoted by α and $w_v^{(i,j)}$ is denoted by w for simplicity), (Shu, Wang, and Cai 2020) reported that these methods tend to lead to a fast converged architecture during the search stage rather than well generalized models. This is because α is updated based on w which is not fully converged rather than well trained w , which is harmful especially in the early epochs. It means that there is a room to search a model with lower error rate in the search space. The proposing MSR-DARTS resolves this issue. It fixes the learnable architecture parameters α to 1 and hence optimizes only w . In the search stage, instead of Eq. (1), the information flow from node i to node j in MSR-DARTS is illustrated in Figure 1 middle bottom, defined as

$$f_{i,j}(x_i) = \sum_{o \in \mathcal{O}} o(x_i). \quad (3)$$

The other process is the same as those defined in Subsec. 2.3.

In MSR-DARTS, we assume that each candidate operator $o_v \in \mathcal{O}$ consists of several convolutional layers. Let c_p^v and c_{fin}^v be the p -th and the last convolutional layers in o_v , respectively. Note that the notation of node (i, j) is omitted for simplicity in c_p^v and c_{fin}^v . Regarding convolutional computation as matrix calculation (Sedghi, Gupta, and Long 2019), $\sigma_q(c_p^v)$ denotes the q -th largest singular value of c_p^v . The stable rank of convolution c is then denoted by $R(c) = \frac{\|c\|_F^2}{\|c\|_2^2}$, where $\|\cdot\|_F$ denotes Frobenius norm and $\|\cdot\|_2$ denotes spectral norm. A stable rank is often used as a surrogate for a rank (Arora et al. 2018).

Then we select the best operator from \mathcal{O} for each edge after training of an over-parameterized network in the search stage. We utilize the relation between network generalization ability and singular values proposed in (Arora et al. 2018). In (Arora et al. 2018), it is reported that a well generalized network consists of noise-robust convolutions which have low stable ranks. Here, noise sensitivity $\psi_{\mathcal{N}}(c, x)$ is defined as

$$\psi_{\mathcal{N}}(c, x) = \mathbb{E}_{\eta \in \mathcal{N}} \left[\frac{\|c(x + \eta\|x\|) - c(x)\|^2}{\|c(x)\|^2} \right], \quad (4)$$

where c is a mapping from real-valued vectors to real-valued vectors (e.g., convolutional computation represented by a

matrix), x is a vector to be multiplied (i.e., input for a convolutional layer), \mathcal{N} is a noise distribution and $\|\cdot\|$ is Euclidean norm. Low noise sensitivity indicates that the convolution matrix has near low rank property (i.e., a low stable rank) because the *signal* x is correctly carried whereas *noise* η is attenuated. Note that noise sensitivity $\psi_{\mathcal{N}}(c, x)$ is at least its stable rank when noise is generated from standard normal distribution, i.e., $\eta \sim \mathcal{N}(0, I)$. For more details, please refer to the paper (Arora et al. 2018).

We assume that an operator that generalizes better has lower noise sensitivity, i.e., a lower stable rank. We further assume that the last convolution c_{fin}^v is the most relevant to the output of the o_v and thus utilize the stable rank of c_{fin}^v (i.e., $R(c_{\text{fin}}^v)$) only. The operator which has the lowest value of $R(c_{\text{fin}}^v)$ is selected to yield the discrete architecture.

3.2 Search Space

DARTS defines an operator set with 8 operators. That is, 3×3 and 5×5 separable convolutions, 3×3 and 5×5 dilated separable convolutions, 3×3 max pooling, 3×3 average pooling, identity, and zero. Our operator set is the subset of the search space of DARTS, i.e., 3×3 and 5×5 separable convolutions, 3×3 and 5×5 dilated separable convolutions. As it is described in Subsec. 3.1, we assume that all candidate operators $o_v \in \mathcal{O}$ consist of limited convolutional layers, where 3×3 max pooling, 3×3 average pooling, identity, and zero, which are not convolutional calculations, are excluded in this study. As in DARTS, we use the ReLU-Conv-BN order for convolutional operators, in which each separable convolution is always applied twice.

3.3 Setting Spectral Norm of Convolution in Search Stage

We assume that in MSR-DARTS, all operators in a search space are trained *correctly* in the search stage. However, (Suzuki, Abe, and Nishimura 2020; Gunasekar et al. 2018; Ji and Telgarsky 2019) reported that deep learning tends to produce a simpler model than its full expression ability when we use regularization such as L_1 regularization. Specifically, it is experimentally shown that a trained network tends to have near low rank weight matrices, in which only a few large singular values and the others are close to zero. Therefore, in each mixed edge of an over-parameterized network in MSR-DARTS, some operators can be redundant because their singular values can be all close to zero. In order to train each operator stably, we apply the spectral norm adjustment technique introduced in (Behrmann et al. 2019) to all convolutional operators in candidate operators, that is,

$$\forall v, p; \|c_p^v\|_2 = C \quad (5)$$

where C is a constant value to be set (Figure 1 right). We estimate the spectral norm of c_p^v by performing power-iteration, which yields an under-estimate $\tilde{\sigma}_1(c_p^v) \leq \|c_p^v\|_2$. Similar to (Behrmann et al. 2019), using this estimate, each convolution in candidate operator c_p^v is normalized as

$$\tilde{c}_p^v = c_p^v \cdot \frac{C}{\tilde{\sigma}_1(c_p^v)}. \quad (6)$$

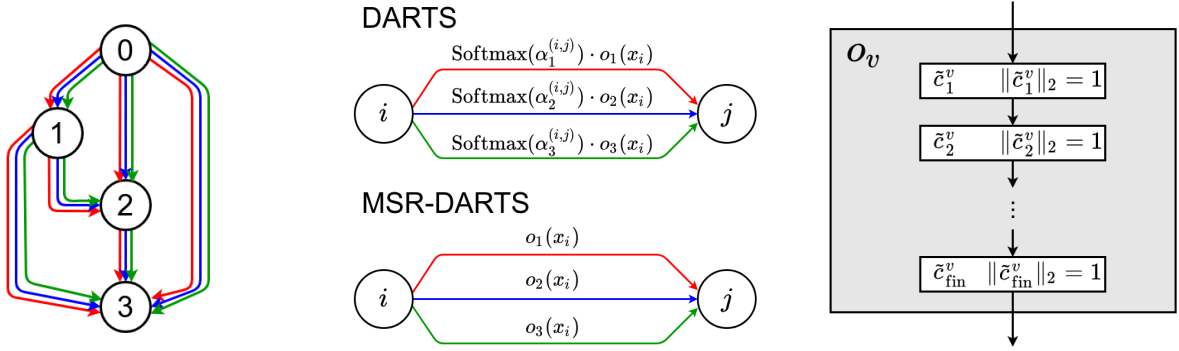


Figure 1: Left: An example of DAG with 4 nodes. Nodes and information flows are illustrated by circles and arrows, respectively. Middle: Difference in the information flow between nodes between DARTS (top) and MSR-DARTS (bottom). Each figure indicates that the number of the candidate operators is 3. Right: Setting the spectral norm of each convolution to a constant value in the search stage.

Note that spectral norm adjustment of each convolution is conducted before forward propagation. $C = 1$ is used in our experiments.

3.4 Deriving Discrete Architecture

After training of the over-parameterized network, a discrete architecture is derived by selecting the topology and the operator for each intermediate node. In DARTS and its derivation, the topology is selected by retaining two strongest precedent edges for each intermediate node, where the strength of an edge from node i to node j is defined as

$$\max_{o \in \mathcal{O}, o \neq \text{zero}} \frac{\exp(\alpha_o^{(i,j)})}{\sum_{o' \in \mathcal{O}} \exp(\alpha_{o'}^{(i,j)})}. \quad (7)$$

In each edge, the operator with the largest α_v is selected. However, as described in Subsec. 3.1, MSR-DARTS uses a fixed value for α_v . We make use of the stable rank of the last convolution $R(c_{\text{fin}}^v)$ in each candidate operator o_v to determine the topology. Specifically, instead of Eq. (7),

$$\min_{o_v \in \mathcal{O}} R(c_{\text{fin}}^v) \quad (8)$$

is used to determine the topology. Note that the operator $o_v \in \mathcal{O}$ which has lower $R(c_{\text{fin}}^v)$ is considered to be a better operator in terms of generalization ability (See Subsec. 3.1). As in DARTS, each intermediate node retain two strongest precedent edges with Eq. (8), and the operator o_v of each edge is determined by

$$\arg \min_v R(c_{\text{fin}}^v). \quad (9)$$

In summary, a discrete architecture is derived from the over-parameterized network after training, where each mixed edge is pruned to an operator according to Eq. (9) and two strongest precedent edges are preserved according to Eq. (8).

4 Experiments

4.1 Datasets

Similar to several previous works (Liu, Simonyan, and Yang 2019; Chen et al. 2019; Xu et al. 2019), we conduct exper-

iments on common image classification datasets, CIFAR-10 (Krizhevsky 2009) and ImageNet (Deng et al. 2009). CIFAR-10 consists of 50,000 training images and 10,000 testing images. All images have fixed size of 32×32 , and these images are equally distributed over 10 classes. ImageNet is obtained from ILSVRC2012 (Russakovsky et al. 2015), which contains 1,000 object classes and 1.28M training images and 50K validation images. We follow the general setting where the input image size is 224×224 .

4.2 Results on CIFAR-10

Following DARTS (Liu, Simonyan, and Yang 2019), the architecture search is conducted on a network with $L = 8$ cells. Each convolutional cell consists of $N = 7$ nodes. The input nodes x_0 and x_1 are equal to the output of the last two preceding cells, respectively. The output node is x_6 which is the concatenation of all the intermediate nodes. Reduction cells are inserted at the 1/3 and 2/3 of the total depth of the network to reduce the spatial resolution of feature maps. All other cells are normal cells which keep the spatial resolution. Note that while DARTS and related works (Xie et al. 2019; Xu et al. 2019) share the architecture topology among all normal cells, the same is true for reduction cells, because they optimize architecture parameters $(\alpha_{\text{normal}}, \alpha_{\text{reduce}})$, where α_{normal} is shared by all the normal cells and α_{reduce} is shared by all the reduce cells (See Subsec. 2.3). On the other hand, each cell has an independent topology in our pipeline because learnable architecture parameters are not optimized in MSR-DARTS.

In the search stage, we split the CIFAR-10 training data in the ratio of four to one. The former is used to train the over-parameterized network weights while the latter is used to calculate the loss. The over-parameterized network is trained for 50 epochs, where the batch size is determined to fit into a single GPU. The initial number of channels is set to be 16. We use momentum SGD to optimize the weights, with initial learning rate 0.025 (annealed down following a cosine schedule), momentum 0.9, and weight decay 3×10^{-4} . We use single TITAN RTX GPU and the architecture search takes less than 0.3 day.

Table 1: Comparison with the state-of-the-art image classifiers on CIFAR-10. Cutout is denoted by c/o.

Architecture	Test Err. (%)	Params (M)	Search Cost (GPU-days)	Search Method
DenseNet-BC (Huang et al. 2017)	3.46	25.6	-	manual
NASNet-A + c/o (Zoph et al. 2018)	2.65	3.3	1800	RL
AmoebaNet-B + c/o (Real et al. 2019)	2.55	2.8	3150	evolution
Hierarchical Evo (Liu et al. 2018b)	3.75	15.7	300	evolution
PNAS (Liu et al. 2018a)	3.41	3.2	225	SMBO
ENAS + c/o (Pham et al. 2018)	2.89	4.6	0.5	RL
DARTS (1st order) + c/o (Liu, Simonyan, and Yang 2019)	3.00	3.3	0.4	gradient-based
DARTS (2nd order) + c/o (Liu, Simonyan, and Yang 2019)	2.76	3.3	1.0	gradient-based
SNAS (moderate) + c/o (Xie et al. 2019)	2.85	2.8	1.5	gradient-based
ProxylessNAS + c/o (Cai, Zhu, and Han 2019)	2.08	-	4.0	gradient-based
DARTS+ + c/o (Liang et al. 2019)	2.20	4.3	0.6	gradient-based
P-DARTS + c/o (Chen et al. 2019)	2.50	3.4	0.3	gradient-based
PC-DARTS + c/o (Xu et al. 2019)	2.57	3.6	0.1	gradient-based
MSR-DARTS + c/o (ours)	2.92	1.7	0.3	gradient-based

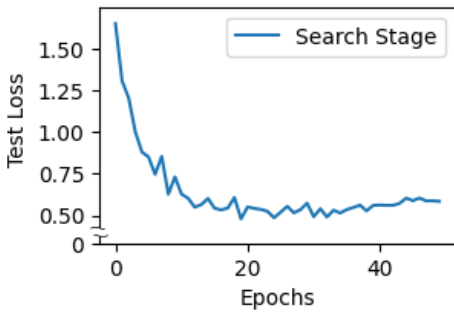


Figure 2: Validation loss transition of the over-parameterized network in the search stage. 50,000 of training images are split into 4:1, the former set is used to optimize network parameters, the latter set is used to validate the network.

In the evaluation stage, the network is composed of 8 cells (6 normal cells and 2 reduce cells). The other settings follow those of DARTS. The network is trained for 600 epochs, with a batch size 96. The initial number of channels is 36, the SGD optimizer with an initial learning rate of 0.025 (annealed down to zero following a cosine schedule), a momentum of 0.9, a weight decay of 3×10^{-4} and gradient clipping at 5. Cutout (DeVries and Taylor 2017), path dropout of probability 0.3, and auxiliary towers with weight 0.4 are used to enhance accuracy.

The validation loss of the over-parameterized network in the search stage is visualized in Figure 2. In the search stage, the validation loss decreases from the beginning of training and takes a minimum value around 25 epochs. On the other hand, validation loss begins to increase little by little after 25 epochs. The architecture generated before the increase in the validation loss is used to the architecture evaluation. Specifically, we use the architecture generated in epoch at

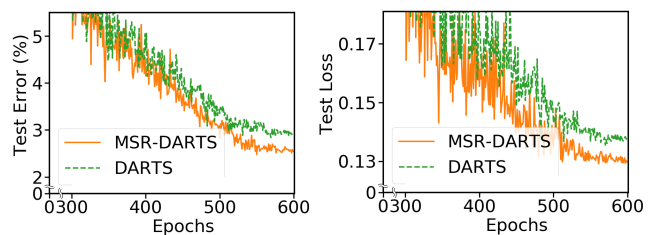


Figure 3: Test error transition (left) and test loss transition (right) of the networks generated by MSR-DARTS and DARTS (after 300 epochs are plotted). Test loss is the average of cross entropy loss over all the test set. Orange solid lines for MSR-DARTS and green dot lines for DARTS.

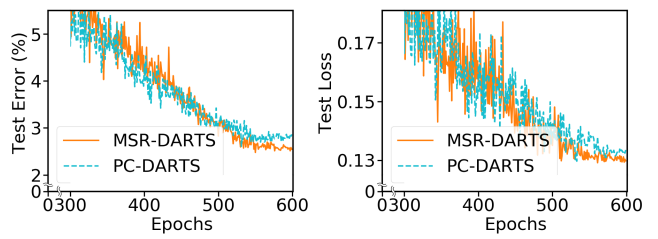


Figure 4: Test error transition (left) and test loss transition (right) of the networks generated by MSR-DARTS and PC-DARTS (after 300 epochs are plotted). Test loss is the average of cross entropy loss over all the test set. Orange solid lines for MSR-DARTS and light blue dot lines for PC-DARTS.

Table 2: Comparison with the other networks under the condition that the number of cells of search stage is the same as that of evaluation stage. We conducted experiments with 8 cells.

Architecture	Test Err. (%)	Search Cost (GPU-days)
DARTS	3.30	1.0
PC-DARTS	3.18	0.1
MSR-DARTS	2.92	0.3

25.

We compare MSR-DARTS to DARTS. Figure 3 left and right indicate the test accuracy and test loss, respectively. Each value is plotted after 300 epochs where the difference can be observed. The architecture generated by MSR-DARTS gets lower test error and higher test accuracy than those by DARTS, which indicates the proposed method outperforms DARTS under the condition that the layer depth on search stage is the same as that of evaluation stage. We also compare our MSR-DARTS to PC-DARTS (Xu et al. 2019). Figure 4 left and right are the comparison of test accuracy and test loss during training respectively. Similar to the comparison between MSR-DARTS and DARTS, we observe that our proposed method demonstrates higher test accuracy and lower test loss after training than those of PC-DARTS, which indicate MSR-DARTS outperforms PC-DARTS under the condition that the layer depth of over-parameterized network on search stage is the same as the depth of the evaluated network.

Table 1 compares the image classification performance of MSR-DARTS with those of the state-of-the-art methods. MSR-DARTS achieves 2.92% test error, which is competitive with or slightly better than the 1st order DARTS. Note that the number of parameters is about 50% of DARTS, and 1.3 times faster than DARTS. Compared to P-DARTS and PC-DARTS, MSR-DARTS found an architecture with much fewer parameters (relative 50% for P-DARTS and 47% for PC-DARTS) with only a slight decrease in accuracy and with almost the same search cost. To the best of our knowledge, the architecture generated by MSR-DARTS has the least parameters that achieves an error rate of less than 3%.

Table 2 summarizes the comparison results on the condition that the numbers of cells are identical during the search stage and the evaluation stage. MSR-DARTS found a model with lower test error compared to DARTS and PC-DARTS. Both architecture search and architecture evaluation are conducted with 8 cells. MSR-DARTS achieves 2.92 test error, which is 0.38% better than DARTS and 0.26% better than PC-DARTS.

4.3 Results on ImageNet

Following DARTS and its derivation, we evaluate the architecture with $L = 14$ cells in the architecture evaluation stage. Since the number of cells in the architecture generated by MSR-DARTS is the same as that in the over-parameterized network in the search stage, the architecture

search for ImageNet is conducted on a network with $L = 14$ cells. CIFAR-10 and ImageNet dataset are used to train an over-parameterized network. In the architecture search using CIFAR-10 dataset, similar to Subsec. 4.2, all the training images are split into 4 : 1. The former set is used to optimize parameters and the latter is used to validate the network. The architecture after epoch 25, which generated the least validation loss in the search phase, is used for the architecture evaluation. A single TITAN RTX GPU is used for the architecture search and it takes less than 0.5 day. In the architecture search using ImageNet dataset, we randomly sample two subsets from the 1.28M training set of ImageNet, with 10% and 2.5% respectively. The former is used for training over-parameterized network weights and the latter for validating the trained network.

In the evaluation stage, the network is composed of 14 cells (12 normal cells and 2 reduction cells). The experimental settings mostly follow DARTS. The network is trained 300 epochs with a batch size 128. The initial number of channels are set to be 48. We use momentum SGD to optimize the weights, with initial learning rate 0.1 (annealed down following a cosine schedule), momentum 0.9, and weight decay 3×10^{-4} . For additional enhancements, label smoothing and an auxiliary loss tower are used during the training. We use 32 Tesla P 100 GPUs, learning warm-up is applied for the first 10 epochs (increase linearly with each batch), Horovod is used for distributed training.

The results are summarized in Table 3. The architecture found by MSR-DARTS using CIFAR-10 dataset reports a top-1 error rate of 24.0% and a top-5 error rate of 7.2%, outperforms the top-1 error rate of 26.7% and the top-5 error rate of 8.7% reported by our baseline DARTS. In the experiments where ImageNet is directly used for the architecture search instead of small proxy dataset such as CIFAR-10, MSR-DARTS reported 24.1% top-1 test error, which outperforms 24.9% of ProxylessNAS and 24.2% of PC-DARTS. It is also a competitive result with 23.9% of DARTS+, with 62% search cost reduction. MSR-DARTS takes only 2.6 GPU-days. To the best of our knowledge, this is the fewest search cost among the state-of-the-art NASs which directly use the ImageNet dataset to optimize the architecture and define search space by directed acyclic graph.

Note that, due to the fact that the search space which includes only limited types of convolutional operators (See Subsec. 3.2), MSR-DARTS has a relatively large number of parameters and of multiply-add operations.

5 Conclusion

We proposed MSR-DARTS, which optimizes only the weight parameters of an over-parameterized network. The discrete architecture selection process using the optimized architecture parameters proposed in DARTS is replaced with the process using a stable rank of each convolution. Utilizing the relation between the generalization ability of neural network and the low-rankness of operator, MSR-DARTS searches for an architecture which is expected to have low test error by selecting the lowest stable rank operator. In our evaluation, MSR-DARTS achieves 2.92% test error on CIFAR-10 and 24.0% test error on ImageNet, both of which

Table 3: Comparison with the state-of-the-art image classifiers on ImageNet. \dagger denotes the architecture was searched on ImageNet directly.

Architecture	Test Err. (%)		Params (M)	$\times +$ (M)	Search Cost GPU-days	Search Method
	top-1	top-5				
Inception-v1 (Szegedy et al. 2015)	30.2	10.1	6.6	1448	-	manual
MobileNet (Howard et al. 2017)	29.4	10.5	4.2	569	-	manual
ShuffleNet 2 \times (v1) (Zhang et al. 2018)	26.4	10.2	5	524	-	manual
ShuffleNet 2 \times (v2) (Ma et al. 2018)	25.1	-	5	591	-	manual
NASNet-A (Zoph et al. 2018)	26.0	8.4	5.3	564	1800	RL
AmoebaNet-C (Real et al. 2019)	24.3	7.6	6.4	570	3150	evolution
PNAS (Liu et al. 2018a)	25.8	8.1	5.1	588	225	SMBO
MnasNet-92 (Tan et al. 2019)	25.2	8.0	4.4	388	-	RL
DARTS (2nd order) (Liu, Simonyan, and Yang 2019)	26.7	8.7	4.7	574	4.0	gradient-based
SNAS (mild) (Xie et al. 2019)	27.3	9.2	4.3	522	1.5	gradient-based
ProxylessNAS(GPU) \dagger (Cai, Zhu, and Han 2019)	24.9	7.5	7.1	465	8.3	gradient-based
DARTS+(CIFAR-100) (Liang et al. 2019)	23.7	7.2	5.1	591	0.2	gradient-based
DARTS+(ImageNet) \dagger (Liang et al. 2019)	23.9	7.4	5.1	582	6.8	gradient-based
P-DARTS(CIFAR-10) (Chen et al. 2019)	24.4	7.4	4.9	557	0.3	gradient-based
P-DARTS(CIFAR-100) (Chen et al. 2019)	24.7	7.5	5.1	577	0.3	gradient-based
PC-DARTS(CIFAR-10) (Xu et al. 2019)	25.1	7.8	5.3	586	0.1	gradient-based
PC-DARTS(ImageNet) \dagger (Xu et al. 2019)	24.2	7.3	5.3	597	3.8	gradient-based
MSR-DARTS(CIFAR-10) (ours)	24.0	7.2	6.7	766	0.5	gradient-based
MSR-DARTS(ImageNet) (ours) \dagger	24.1	7.7	6.6	748	2.6	gradient-based

is accomplished within 0.5 GPU-days. It is also possible for MSR-DARTS to search an architecture for ImageNet by directly using ImageNet dataset. It takes only 2.6 days on single GPU, which is the state-of-the-art search cost while the accuracies keep competitive results among the architecture search methods which directly use the ImageNet dataset to optimize architecture and define the search space by directed acyclic graph.

Acknowledgements

This work was supported by JST CREST JPMJCR1687. TS was partially supported by MEXT Kakenhi (15H05707, 18K19793 and 18H03201), and Japan Digital Design.

References

Ahn, N.; Kang, B.; and Sohn, K.-A. 2018. Fast, accurate, and lightweight super-resolution with cascading residual network. In *Proceedings of the European Conference on Computer Vision (ECCV)*, 252–268.

Arora, S.; Ge, R.; Neyshabur, B.; and Zhang, Y. 2018. Stronger Generalization Bounds for Deep Nets via a Compression Approach. In Dy, J. G.; and Krause, A., eds., *Proceedings of the 35th International Conference on Machine Learning, ICML 2018, Stockholm, Sweden, July 10-15, 2018*, volume 80 of *Proceedings of Machine Learning Research*, 254–263. PMLR. URL <http://proceedings.mlr.press/v80/arora18b.html>.

Bartlett, P. L.; and Mendelson, S. 2002. Rademacher and Gaussian complexities: Risk bounds and structural results. *Journal of Machine Learning Research* 3(Nov): 463–482.

Baykal, C.; Liebenwein, L.; Gilitschenski, I.; Feldman, D.; and Rus, D. 2019. Data-Dependent Coresets for Compressing Neural Networks with Applications to Generalization Bounds. In *7th International Conference on Learning Representations, ICLR 2019, New Orleans, LA, USA, May 6-9, 2019*. OpenReview.net. URL <https://openreview.net/forum?id=HJfwJ2A5KX>.

Behrmann, J.; Grathwohl, W.; Chen, R. T. Q.; Duvenaud, D.; and Jacobsen, J. 2019. Invertible Residual Networks. In Chaudhuri, K.; and Salakhutdinov, R., eds., *Proceedings of the 36th International Conference on Machine Learning, ICML 2019, 9-15 June 2019, Long Beach, California, USA*, volume 97 of *Proceedings of Machine Learning Research*, 573–582. PMLR. URL <http://proceedings.mlr.press/v97/behrmann19a.html>.

Cai, H.; Zhu, L.; and Han, S. 2019. ProxylessNAS: Direct Neural Architecture Search on Target Task and Hardware. In *7th International Conference on Learning Representations, ICLR 2019, New Orleans, LA, USA, May 6-9, 2019*. OpenReview.net. URL <https://openreview.net/forum?id=HyIVB3AqYm>.

Chen, X.; Xie, L.; Wu, J.; and Tian, Q. 2019. Progressive differentiable architecture search: Bridging the depth gap between search and evaluation. In *Proceedings of the IEEE International Conference on Computer Vision*, 1294–1303.

Deng, J.; Dong, W.; Socher, R.; Li, L.-J.; Li, K.; and Fei-Fei, L. 2009. ImageNet: A Large-Scale Hierarchical Image Database. In *CVPR09*.

DeVries, T.; and Taylor, G. W. 2017. Improved regulariza-

tion of convolutional neural networks with cutout. *arXiv preprint arXiv:1708.04552* .

Dziugaite, G. K.; and Roy, D. M. 2017. Computing nonvacuous generalization bounds for deep (stochastic) neural networks with many more parameters than training data. *arXiv preprint arXiv:1703.11008* .

Golowich, N.; Rakhlin, A.; and Shamir, O. 2018. Size-independent sample complexity of neural networks. In *Conference On Learning Theory*, 297–299.

Gunasekar, S.; Lee, J. D.; Soudry, D.; and Srebro, N. 2018. Implicit Bias of Gradient Descent on Linear Convolutional Networks. In Bengio, S.; Wallach, H. M.; Larochelle, H.; Grauman, K.; Cesa-Bianchi, N.; and Garnett, R., eds., *Advances in Neural Information Processing Systems 31: Annual Conference on Neural Information Processing Systems 2018, NeurIPS 2018, 3-8 December 2018, Montréal, Canada*, 9482–9491. URL <http://papers.nips.cc/paper/8156-implicit-bias-of-gradient-descent-on-linear-convolutional-networks>.

Harvey, N.; Liaw, C.; and Mehrabian, A. 2017. Nearly-tight VC-dimension bounds for piecewise linear neural networks. In Kale, S.; and Shamir, O., eds., *Proceedings of the 2017 Conference on Learning Theory*, volume 65 of *Proceedings of Machine Learning Research*, 1064–1068. Amsterdam, Netherlands: PMLR. URL <http://proceedings.mlr.press/v65/harvey17a.html>.

Howard, A. G.; Zhu, M.; Chen, B.; Kalenichenko, D.; Wang, W.; Weyand, T.; Andreetto, M.; and Adam, H. 2017. MobileNets: Efficient Convolutional Neural Networks for Mobile Vision Applications. *CoRR* abs/1704.04861. URL <http://arxiv.org/abs/1704.04861>.

Huang, G.; Liu, Z.; van der Maaten, L.; and Weinberger, K. Q. 2017. Densely Connected Convolutional Networks. In *Proceedings of the IEEE Conference on Computer Vision and Pattern Recognition (CVPR)*.

Ji, Z.; and Telgarsky, M. 2019. Gradient descent aligns the layers of deep linear networks. In *7th International Conference on Learning Representations, ICLR 2019, New Orleans, LA, USA, May 6-9, 2019*. OpenReview.net. URL <https://openreview.net/forum?id=HJflg30qKX>.

Krizhevsky, A. 2009. Learning multiple layers of features from tiny images. Technical report.

Liang, H.; Zhang, S.; Sun, J.; He, X.; Huang, W.; Zhuang, K.; and Li, Z. 2019. Darts+: Improved differentiable architecture search with early stopping. *arXiv preprint arXiv:1909.06035* .

Liu, C.; Chen, L.-C.; Schroff, F.; Adam, H.; Hua, W.; Yuille, A. L.; and Fei-Fei, L. 2019. Auto-deeplab: Hierarchical neural architecture search for semantic image segmentation. In *Proceedings of the IEEE conference on computer vision and pattern recognition*, 82–92.

Liu, C.; Zoph, B.; Neumann, M.; Shlens, J.; Hua, W.; Li, L.-J.; Fei-Fei, L.; Yuille, A.; Huang, J.; and Murphy, K. 2018a. Progressive Neural Architecture Search. In *Proceedings of the European Conference on Computer Vision (ECCV)*.

Liu, H.; Simonyan, K.; Vinyals, O.; Fernando, C.; and Kavukcuoglu, K. 2018b. Hierarchical Representations for Efficient Architecture Search. In *6th International Conference on Learning Representations, ICLR 2018, Vancouver, BC, Canada, April 30 - May 3, 2018, Conference Track Proceedings*. OpenReview.net. URL <https://openreview.net/forum?id=BJQRKzbA->.

Liu, H.; Simonyan, K.; and Yang, Y. 2019. DARTS: Differentiable Architecture Search. In *International Conference on Learning Representations*. URL <https://openreview.net/forum?id=S1eYHoC5FX>.

Ma, N.; Zhang, X.; Zheng, H.-T.; and Sun, J. 2018. ShuffleNet V2: Practical Guidelines for Efficient CNN Architecture Design. In *Proceedings of the European Conference on Computer Vision (ECCV)*.

Neyshabur, B.; Bhojanapalli, S.; and Srebro, N. 2017. A pac-bayesian approach to spectrally-normalized margin bounds for neural networks. *arXiv preprint arXiv:1707.09564* .

Neyshabur, B.; Salakhutdinov, R. R.; and Srebro, N. 2015. Path-SGD: Path-Normalized Optimization in Deep Neural Networks. In Cortes, C.; Lawrence, N. D.; Lee, D. D.; Sugiyama, M.; and Garnett, R., eds., *Advances in Neural Information Processing Systems 28*, 2422–2430. Curran Associates, Inc. URL <http://papers.nips.cc/paper/5797-path-sgd-path-normalized-optimization-in-deep-neural-networks.pdf>.

Pham, H.; Guan, M. Y.; Zoph, B.; Le, Q. V.; and Dean, J. 2018. Efficient Neural Architecture Search via Parameter Sharing. In Dy, J. G.; and Krause, A., eds., *Proceedings of the 35th International Conference on Machine Learning, ICML 2018, Stockholm, Sweden, July 10-15, 2018*, volume 80 of *Proceedings of Machine Learning Research*, 4092–4101. PMLR. URL <http://proceedings.mlr.press/v80/pham18a.html>.

Real, E.; Aggarwal, A.; Huang, Y.; and Le, Q. V. 2019. Regularized Evolution for Image Classifier Architecture Search. In *The Thirty-Third AAAI Conference on Artificial Intelligence, AAAI 2019, The Thirty-First Innovative Applications of Artificial Intelligence Conference, IAAI 2019, The Ninth AAAI Symposium on Educational Advances in Artificial Intelligence, EAAI 2019, Honolulu, Hawaii, USA, January 27 - February 1, 2019*, 4780–4789. AAAI Press. doi:10.1609/aaai.v33i01.33014780. URL <https://doi.org/10.1609/aaai.v33i01.33014780>.

Russakovsky, O.; Deng, J.; Su, H.; Krause, J.; Satheesh, S.; Ma, S.; Huang, Z.; Karpathy, A.; Khosla, A.; Bernstein, M.; Berg, A. C.; and Fei-Fei, L. 2015. ImageNet Large Scale Visual Recognition Challenge. *International Journal of Computer Vision (IJCV)* 115(3): 211–252. doi:10.1007/s11263-015-0816-y.

Sedghi, H.; Gupta, V.; and Long, P. M. 2019. The Singular Values of Convolutional Layers. In *7th International Conference on Learning Representations, ICLR 2019, New Orleans, LA, USA, May 6-9, 2019*. OpenReview.net. URL <https://openreview.net/forum?id=rJevYoA9Fm>.

Shu, Y.; Wang, W.; and Cai, S. 2020. Understanding Architectures Learnt by Cell-based Neural Architecture Search. In *8th International Conference on Learning Representations, ICLR 2020, Addis Ababa, Ethiopia, April 26-30, 2020*. OpenReview.net. URL <https://openreview.net/forum?id=BJxH22EKPS>.

Suzuki, T.; Abe, H.; and Nishimura, T. 2020. Compression based bound for non-compressed network: unified generalization error analysis of large compressible deep neural network. In *8th International Conference on Learning Representations, ICLR 2020, Addis Ababa, Ethiopia, April 26-30, 2020*. OpenReview.net. URL <https://openreview.net/forum?id=ByeGzlrKwH>.

Szegedy, C.; Liu, W.; Jia, Y.; Sermanet, P.; Reed, S.; Anguelov, D.; Erhan, D.; Vanhoucke, V.; and Rabinovich, A. 2015. Going Deeper With Convolutions. In *Proceedings of the IEEE Conference on Computer Vision and Pattern Recognition (CVPR)*.

Tan, M.; Chen, B.; Pang, R.; Vasudevan, V.; Sandler, M.; Howard, A.; and Le, Q. V. 2019. MnasNet: Platform-Aware Neural Architecture Search for Mobile. In *Proceedings of the IEEE/CVF Conference on Computer Vision and Pattern Recognition (CVPR)*.

Tang, J.; Golbabaei, M.; and Davies, M. E. 2017. Gradient Projection Iterative Sketch for Large-Scale Constrained Least-Squares. In Precup, D.; and Teh, Y. W., eds., *Proceedings of the 34th International Conference on Machine Learning, ICML 2017, Sydney, NSW, Australia, 6-11 August 2017*, volume 70 of *Proceedings of Machine Learning Research*, 3377–3386. PMLR. URL <http://proceedings.mlr.press/v70/tang17a.html>.

Vapnik, V. N. 1998. *Statistical Learning Theory*. Wiley-Interscience.

Xie, S.; Zheng, H.; Liu, C.; and Lin, L. 2019. SNAS: stochastic neural architecture search. In *7th International Conference on Learning Representations, ICLR 2019, New Orleans, LA, USA, May 6-9, 2019*. OpenReview.net. URL <https://openreview.net/forum?id=rylqooRqK7>.

Xu, Y.; Xie, L.; Zhang, X.; Chen, X.; Qi, G.-J.; Tian, Q.; and Xiong, H. 2019. Pcdarts: Partial channel connections for memory-efficient differentiable architecture search. *arXiv preprint arXiv:1907.05737*.

Zhang, X.; Zhou, X.; Lin, M.; and Sun, J. 2018. ShuffleNet: An Extremely Efficient Convolutional Neural Network for Mobile Devices. In *2018 IEEE Conference on Computer Vision and Pattern Recognition, CVPR 2018, Salt Lake City, UT, USA, June 18-22, 2018*, 6848–6856. IEEE Computer Society. doi:10.1109/CVPR.2018.00716. URL http://openaccess.thecvf.com/content_cvpr_2018/html/Zhang_ShuffleNet_An_Exremely_CVPR_2018_paper.html.

Zoph, B.; and Le, Q. V. 2017. Neural Architecture Search with Reinforcement Learning. In *5th International Conference on Learning Representations, ICLR 2017, Toulon, France, April 24-26, 2017, Conference Track Proceedings*. OpenReview.net. URL <https://openreview.net/forum?id=r1Ue8Hcxg>.

Zoph, B.; Vasudevan, V.; Shlens, J.; and Le, Q. V. 2018. Learning transferable architectures for scalable image recognition. In *Proceedings of the IEEE conference on computer vision and pattern recognition*, 8697–8710.